Conductance of quantum point contact

Guanglei Wang, Dragica Vasileska

***Abstract*—The classic Landauer's formula relates the conductance of a quantum point contact or wire to transmission probabilities. There are mainly two approaches to calculate the conductance based on this formula: the Green's function techniques and the mode matching techniques. The Green's function approach is frequently used to calculate the total transmission probabilities while the mode matching approach, which is based on the scattering wavefunction, is normally exploited to calculate the partial transmission probabilities. In this final project of ASU EEE532, Spring 2015, we try to learn the mode matching approach formulated by Ando [Phys.Rev. B 44 , 8017 (1991)] [1]. We calculate the conductance of a quantum point contact under a confinement potential as well as the gate voltage. We also consider the effects of short-range disorders. The results show clear quantum quantization phenomenon for the quantum point contact and we discuss several issues that affect the quantized behavior.**

***Keywords*—Transfer matrix, Green's function, quantum point contact.**

I. Introduction

The developments of fabrication technology have made it possible to obtain quantum ballistic structure of nanoscale, where the quantum effects can be dominated. Because the small scale of the device, its transport behavior should be understood based on a atom level theory. Landauer-Buttiker approach is such a classic theory to relate the conductance with the transmission probabilities within the linear response regime. Normally, both the Green's function and mode matching technicals are used to calculate the conductance. And the two technicals have been proved to be equivalent. In Green's function technical, a small imaginary part must be added to the energy to distinguish between the retarded and advanced Green's function while the energy used in the mode matching technical is totally real. The mode matching technical is formulated by Ando, which is based on matching the wavefunction in the scattering regime to the Bloch modes of the lead. In this way we can easily calculate the transmission of each mode. Considering the advantages of the mode matching technical and its widely using, in this final project, we try to learn the basic knowledge of the mode matching technical and use it to calculate the quantum conductance of a quantum point contact.

This report is organized as follows. In Sec.II, we briefly introduce the form of Hamiltonian in the lattice model under the tight-binding approximation. We consider the situation of the ideal wire, the scattering wire and talk about detail approaches of calculations. In Sec.III, we show our results of the behavior of the conductance under the variation of some system parameters. The main conclusions are made in Sec.IV.

G.-L. Wang is a graduate student of the School of Electrical, Computer, and Energy Engineering, Arizona State University, Tempe, AZ, 85287 USA e-mail: glwang@asu.edu.

D. Vasileska is a professor of the School of Electrical, Computer, and Energy Engineering, Arizona State University, Tempe, AZ, 85287 USA e-mail: vasileska@asu.edu.

II. Model

We consider a square lattice with lattice constant a under the tight-binding approximation. Each atom has a pair of coordinates (i, j) to represent its position. The nearest-neighbor interaction is characterized by the transfer integral, $-t$. In this report we use $t = E_F(\frac{1}{2\pi})^2(\frac{\lambda_F}{a})^2$. If the system is under the effect of magnetic field with Landau gauge, the interaction Hamiltonian of the system can be written as

$$\begin{aligned}\langle l, j|\mathcal{H}|l+1, j\rangle &= -texp(2\pi i\tilde{H}j)\\ \langle l, j|\mathcal{H}|l, j+1\rangle &= -t,\end{aligned} \tag{1}$$

where there is a so-called Peierls phase factor $exp(2\pi i\tilde{H}j), j = 1, \ldots, M$. Here the strength of magnetic field is introduced through $\tilde{H} = \Phi/\Phi_0$ with $\Phi = Ha^2$ being the magnetic flux across a unit cell and $\Phi_0 = ch/e$ is the magnetic flux quantum. The magnetic field is expressed as $\tilde{H} = \pi\frac{\hbar\omega_c}{E_F}(\frac{a}{\lambda_F})^2$. The on-site energy is expressed as the diagonal element of the Hamiltonian which is written as

$$\langle l, j|\mathcal{H}|l, j\rangle = 4t + v(l, j), \tag{2}$$

where the first term on the right hand side is nothing but a shift of the total energy and the second term denotes the confinement energy. To consider the effect of short-range disorders, we can just add an random potential to each diagonal element of the Hamiltonian. The strength of the random disorder is within $[-W/2, W/2]$. Here we have

$$\frac{W}{E_F} = (\frac{6\lambda_F^3}{\pi^3 a^2\Lambda})^{1/2}, \tag{3}$$

where Λ is the mean free path of the electrons.

A. Ideal wire

The simplest situation we can have in the quantum transport problem is an ideal wire, i.e., $v(l, j) = 0$ for all the lattice points. Suppose the ideal wire is infinite along the x direction but is consisted of M lattice sites in the y direction. As we are under the tight-binding approximation, the equation of motion can be described as

$$(E - \mathcal{H}_0)\psi_i + tP\psi_{i-1} + tP^*\psi_{i+1} = 0, \tag{4}$$

where ψ_i is a vector of the amplitudes of the ith cell and P is the coupling Hamiltonian between the nearest cells:

$$P_{ll'} = exp(2\pi i\tilde{H}l)\delta_{l,l'}, \tag{5}$$

where $l, l' = 1, \ldots, M$.

As in the ideal wire, the Hamiltonian for each single slice is the same, i.e., $\mathcal{H}_0$, which is also an $M \times M$ matrix:

$$\mathcal{H}_0 = \begin{bmatrix} v_1 + 4t & -t & 0 & \ldots & 0 \\ -t & v_2 + 4t & -t & \ldots & 0 \\ 0 & -t & v_3 + 4t & \ldots & 0 \\ \vdots & \vdots & \vdots & \ddots & \vdots \\ 0 & 0 & 0 & \ldots & v_M + 4t \end{bmatrix}. \tag{6}$$

The advantage of the ideal wire is that the Bloch theorem can be easily used, i.e., the wavefunction should be constructed by a function which has the same period as the potential multiplies an envelop modulation. So we can assume

$$\psi_i = \lambda^i \psi_0. \tag{7}$$

Then from the equation of motion we can have

$$\lambda \psi_i = t^{-1} P(\mathcal{H}_0 - E)\psi_i - P^2 \psi_{i-1},$$

which can lead to a $2M \times 2M$ eigenvalue problem:

$$\lambda \begin{bmatrix} \psi_i \\ \psi_{i-1} \end{bmatrix} = \begin{bmatrix} t^{-1}P(\mathcal{H}_0 - E) & -P^2 \\ I & 0 \end{bmatrix} \begin{bmatrix} \psi_i \\ \psi_{i-1} \end{bmatrix}. \tag{8}$$

Here in the above equation, E is understood as the chemical potential which can be setup through the gate voltage. For a given gate energy E, we can have an eigenvalue problem which can result in $2M$ eigenvalues and $2M$ eigenvectors. The dimension of the eigenvector is $2M \times 1$ which comes from the fact that the above equation couples ψ_i and ψ_{i+1}, and each of them is of dimension $M \times 1$. Based on the form of our equation, the first M elements of the eigenvector belong to ψ_i and the following M elements belong to ψ_{i-1}. The origin of the $2M$ eigenvalues is that we should have M left-going and M right-going waves. Of course, there should be propagating modes and evanescent modes. One can distinguish right- and left-going evanescent modes based on the magnitudes of these corresponding eigenvalues, i.e., right-going evanescent modes have $|\lambda(+)| < 1$ and left-going evanescent modes have $|\lambda(-)| > 1$. However, one can not tell the direction of the propagating modes directly through the eigenvalues or wave vectors. Actually, the quantity that is concerned is the group velocity. Propagating modes have unit eigenvalue magnitude but different signs of group velocities [2], [3]. The group velocity for a given mode is expressed as [2]

$$v_n(\pm) = -\frac{2a}{\hbar} Im[\lambda_n(\pm)\mathbf{u}_n(\pm)^\dagger \mathcal{H}^\dagger_{i,i+1}\mathbf{u}_n(\pm)], \tag{9}$$

so the right propagating mode has positive group velocity while the left propagating mode has a negative one.

After distinguishing the left- and right-going modes we can construct some useful matrices, which are

$$U(\pm) = (\mathbf{u}_1(\pm), \ldots, \mathbf{u}_M(\pm)) \tag{10}$$

and

$$\Lambda(\pm) = \begin{bmatrix} \lambda_1(\pm) & \ldots & 0 \\ \vdots & \ddots & \vdots \\ 0 & \ldots & \lambda_M(\pm) \end{bmatrix}. \tag{11}$$

Here the matrix $U(\pm)$ is nothing but a group of eigenvectors for the right(left) going modes. We will later see that it is used to calculate how much transmission each mode contributes. At last we need to define

$$F(\pm) = U(\pm)\Lambda(\pm)U^{-1}(\pm). \tag{12}$$

B. Scattering problem

After obtaining the transport modes for the ideal wire, we now move on to the scattering problem. The scattering can be as simple as the effect of the confinement potential. When the potential profile of the device is not uniform, the states of electrons will be disturbed, i.e., scattering will happen. The basic approach to deal with this scattering in the mode matching technical [4] is to calculate the relation of the out-going waves with the in-going waves. For example, if we concern transmission, we should focus on the right propagating waves on the most left and right parts of device. If we consider the reflection, we should focus on the left propagating waves on the most left part of the device. Normally, we assume the leads are semi-infinite and ideal and the length of the scattering regime is N, i.e., is consisted of N lattice points.

To be concrete, we consider the interface of the left lead and the device

$$\psi_0 = \psi_0(+) + \psi_0(-). \tag{13}$$

And we can also relate ψ_{-1} to ψ_0 through the $F(\pm)$ matrices

$$C_{-1} = F^{-1}(+)\psi_0(+) + F^{-1}(-)\psi_0(-). \tag{14}$$

Then we can exploit the equation of motion at cell 0 to get

$$(E - \tilde{\mathcal{H}}_0)\psi_0 = tP^*\psi_1 = -tP[F^{-1}(+) - F^{-1}(-)]\psi_0(+), \tag{15}$$

where

$$\tilde{\mathcal{H}}_0 = \mathcal{H}_0 - tPF^{-1}(-). \tag{16}$$

Similarly, for the most right part of the device we can have

$$(E - \tilde{\mathcal{H}}_{N+1})\psi_{N+1} + tP\psi_N = 0, \tag{17}$$

where

$$\tilde{\mathcal{H}}_{N+1} = \mathcal{H}_{N+1} - tP^*F(+). \tag{18}$$

Here $\tilde{\mathcal{H}}_0$ and $\tilde{\mathcal{H}}_{N+1}$ actually already contain the effects coming from the two semi-infinite leads. We should notice that the right hand side of Eq.15 is not 0. Indeed, the term $-tP[F^{-1}(+) - F^{-1}(-)]\psi_0(+)$ serves as a source of the current.

To calculate the effect of the source term on the most right part of the device, we can use the Green's function technical. Here, we should emphasis that the Green's function used here is just a tool to calculate the wavefunction on the most right side of the device, after which we should use mode matching technicals to match the wavefunction to the eigenfunctions of the ideal leads. We can define the Green's function G as

$$G = \frac{1}{E - \tilde{\mathcal{H}}}, \tag{19}$$

with

$$\tilde{\mathcal{H}} = \begin{bmatrix} \tilde{\mathcal{H}}_0 & -tP^* & 0 & \dots & 0 & 0 \\ -tP & \tilde{\mathcal{H}}_1 & -tP^* & \dots & 0 & 0 \\ 0 & -tP & \tilde{\mathcal{H}}_2 & \dots & 0 & 0 \\ \vdots & \vdots & \vdots & \ddots & \vdots & \vdots \\ 0 & 0 & 0 & \dots & \tilde{\mathcal{H}}_N & -tP^* \\ 0 & 0 & 0 & \dots & -tP & \tilde{\mathcal{H}}_{N+1} \end{bmatrix}. \quad (20)$$

The role of the source is reflected in the coupling of ψ_0 and ψ_{N+1}

$$\begin{aligned} \psi_{N+1}(+) &= \psi_{N+1} \\ &= -t\langle N+1|G|0\rangle P[F^{-1}(+) - F^{-1}(-)]\psi_0(+). \end{aligned} \quad (21)$$

From which the transmission coefficient $t_{\mu\nu}$ for the incident channel ν to the out-going channel μ is

$$\begin{aligned} t_{\mu\nu} =& (\frac{v_\mu}{v_\nu})^{1/2}\{-tU^{-1}(+)\langle N+1|G|0\rangle \\ & \times P[F^{-1}(+) - F^{-1}(-)]U(+)\}_{\mu\nu}, \end{aligned} \quad (22)$$

where v_ν and v_μ are the velocity for each channel, respectively.

C. Recursive formulas

As there are matrix inverse manipulations in the calculations of Green's function, we can exploit an recursive formulas to speed up the calculation. The essence of this formulas is to replace the inverse of a very large matrix (the same dimension as the number of atoms in the device) with many inverses of small matrices (the same dimension as the number of atoms in the slice) [5]. To be concrete, in our device , the recursive formulas is

$$\begin{aligned} &\langle i+1|G^{(i+1)}|i+1\rangle^{-1} \\ &\qquad = E - \tilde{\mathcal{H}}_{i+1} - \tilde{\mathcal{H}}_{i+1,i}\langle i|G^{(i)}|i\rangle\tilde{\mathcal{H}}_{i,i+1}, \\ &\langle i+1|G^{(i+1)}|0\rangle \\ &\qquad = \langle i+1|G^{(i+1)}|i+1\rangle\tilde{\mathcal{H}}_{i+1,i}\langle i|G^{(i)}|0\rangle, \end{aligned} \quad (23)$$

the initial condition is $\langle 0|G^{(0)}|0\rangle = (E - \tilde{\mathcal{H}}_0)^{-1}$.

III. Results

We consider a wire with length L_x and width L_y and under the influence of a confinement potential

$$\begin{aligned} V(x,y) =& \frac{V}{2}[1 + cos(\frac{2\pi x}{L_x})] \\ &+ E_F(\frac{y - y_+(x)}{\Delta})^2\theta(y - y_+(x)) \\ &+ E_F(\frac{y - y_-(x)}{\Delta})^2\theta(-(y - y_-(x))), \end{aligned} \quad (24)$$

where $\theta(t)$ is a step function and

$$y_\pm(x) = \pm\frac{L_y}{4}[1 - cos(\frac{2\pi x}{L_x})]. \quad (25)$$

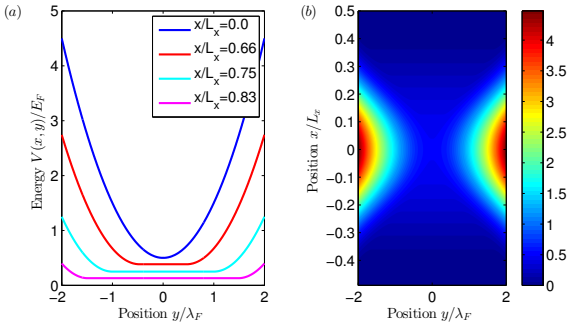

Fig. 1. An example of the confinement potential profile used to simulate a quantum point contact. (a) Confinement potential along y direction under several different x positions. (b) A contour view of the confinement potential of the quantum point contact. Note that the scale for the x and y axises are different. The other parameters are $V/E_F = 0.5$, $\Delta/\lambda_F = 1$, and $L_y/\lambda_F = 4$. The solid lines in (a) represents the potential profile at $x/L_x = 0, 0.66, 0.75, 0.83$.

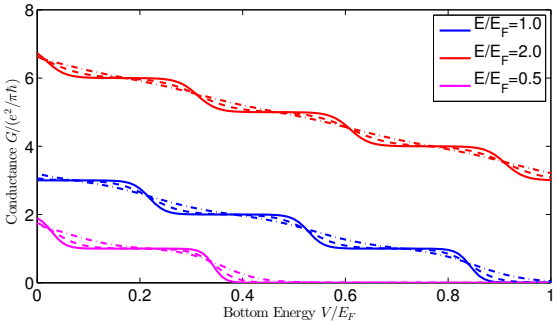

Fig. 2. Total conductance through a quantum point contact under different bottom energy V/E_F. The lines with different colors represent different gate voltage, i.e., red: $E/E_F = 1.0$, blue: $E/E_F = 2.0$, pink: $E/E_F = 0.5$. The different line styles represents different length of the quantum point contact, i.e., solid: $L_x/\lambda_F = 16.0$, dash: $L_x/\lambda_F = 8.0$, dash-dot: $L_x/\lambda_F = 4.0$

In Fig.1 we show a typical profile of this confinement potential. Fig.1 (a) is the example of the confinement potential under some different x positions. The minimum energy under $x/L_x = 0$ is called the bottom energy. Fig.1 (b) is a contour figure of the confinement potential all over the device. We use a much smaller mesh than that used in simulation to show the detail of this confinement.

Fig.2 shows the dependence of the total conductance of the quantum point contact on the bottom energy, V/E_F. The red, blue and pink curves are correspondening to the gate energy $E/E_F = 2.0, 1.0, 0.5$, respectively. For the different line styles under the same color, they represent different lengths of the device. The blue lines are the same as that in the work of T. Ando's, which proves the valid of our program. We can see that for a rather long device, there is a very clear conductance quantization phenomenon. We can see the conductance steps obviously. However, when the length of the device becomes smaller, the conductance becomes less quantized as the potential variation is far from being adiabatic. Furthermore, we can also see that the gate voltage also plays

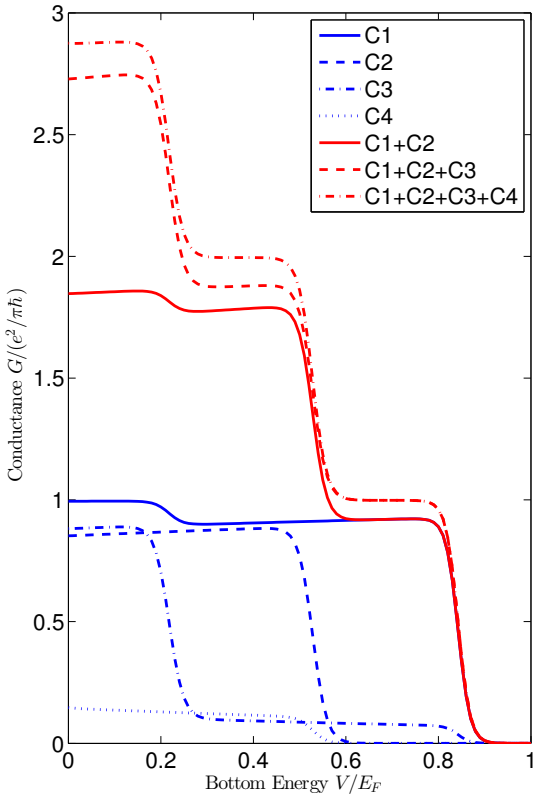

Fig. 3. Conductance distribution among out-going channels as a function of the bottom energy V/E_F through the quantum point contact. The blue curves are conductances for different single channels and the red curves are for sum channels. C_i denotes channel i with $i = 1, 2, 3, 4$. The gate energy used here is $E/E_F = 1.0$ so that there are four propagating modes in the ideal lead.

a significant role here. When the gate energy, or the chemical potential, is high, there should be more propagating modes in the leads, which increases the conductance. Another physical picture to understand this is through the band structure. As we increase the gate voltage, the chemical potential will have more crosses with the band structure, and more crosses mean more transporting modes. In Fig.2, we can also see the effect of the bottom energy very well. We can see that for a long device, a bottom energy which is lower than the gate energy is high enough to block the transport of the device. However, for a short device, it is reasonable that the transport should be robust than that of the long one.

To exploit the advantage of the mode matching approach, we show the quantum conductance for each mode separately in Fig.3. It shows the detail of the variation of each propagating mode with the change of the bottom energy. It clearly shows that the conductance can not go beyond $e^2/\pi\hbar$ for one channel, which results from the Fermi property, or the Pauli exclusion principle, of electrons. We can see that when the bottom energy becomes higher and the total conductance jumps to a lower

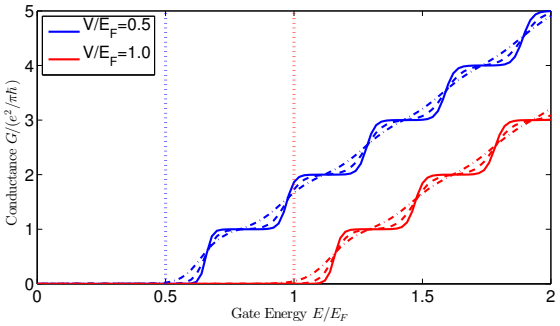

Fig. 4. Total conductance through a quantum point contact under different gate energy E/E_F. The lines with different colors represent different bottom energy, i.e., red: $V/E_F = 1.0$, blue: $V/E_F = 0.5$. The different line styles represents different length of the quantum point contact, i.e., solid: $L_x/\lambda_F = 16.0$, dash: $L_x/\lambda_F = 8.0$, dash-dot: $L_x/\lambda_F = 4.0$

value, the conductance of the highest channel jumps from close to unity to close one. This is because the confinement potential blocks the transport of that channel. Another interesting phenomenon is that the conductance of the very high channel's can keep finite, even close to zero, within a rather large bottom energy regime.

Except the dependence of the conductance on the bottom energy, we also show the relation of the conductance with the gate energy E/E_F. The results are shown in Fig.4. We do two groups of simulations with the bottom energy $V/E_F = 0.5, 1.0$ and also under three different device lengths. From Fig.4, we can see a typical ribbon conductance behavior. The conductance starts to appear above the bottom energy of each case, which is shown by the vertical dot line. Again, the length of the device can change the quantization behavior. The detail variation of each channel is shown in Fig.5. An interesting behavior of the channel conductance is that there is a trend to decrease after it reaches the maximum value, i.e., one, and then increases back to unity. Also, from the behavior of the single channel, we can inform the minimum energy of several bands in the band structure.

Another interesting question is the effect of disorders on the conductance of the quantum point contact. Of course, there are many kinds of disorders, and here we use the simplest one, i.e., the short-range random disorder. Mathematically, we just need to add a random potential to each diagonal element of the Hamiltonian. The simulation results are shown in Fig.6 and Fig.7 with the variation of the bottom energy and gate energy, respectively. For each case, we make 100 realizations of the random disorder with the same strength, W. The strength of the disorder is characterized by the mean free path Λ. The blue dots are for $\Lambda/\lambda_F = 200.0$ and the red dots are for $\Lambda/\lambda_F = 20.0$, where a larger mean free path denotes a weaker disorder. The results are agreed with the expectation. There is a clear signature that the blue dots are more focused than the red dots. And a stronger disorder can even destroy the quantization of the conductance. Again, the gate energy we used in Fig.6 is $E/E_F = 1.0$ and the bottom energy we used in Fig.7 is $V/E_F = 0.5$.

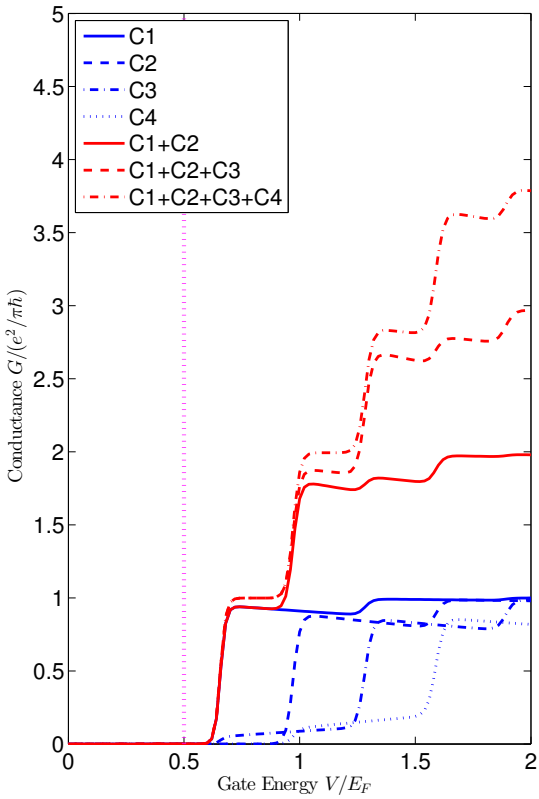

Fig. 5. Conductance distribution among out-going channels as a function of the gate energy E/E_F through the quantum point contact. The blue curves are conductances for different single channels and the red curves are for sum channels. C_i denotes channel i with $i = 1, 2, 3, 4$. When the gate energy is higher than E_F, more propagating modes can be existed in the quantum point contact. Here we just show the first four channels.

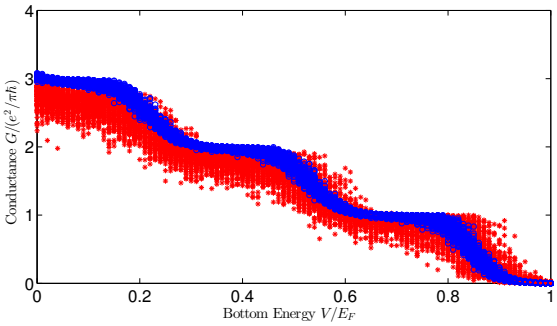

Fig. 6. Examples of the conductances through a quantum point contact as a function of the bottom energy under the effect of short-range disorders characterized by the mean free path Λ. Here we show 100 realizations of the random disorders with $\Lambda/\lambda_F = 200.0$, blue dots, and $\Lambda/\lambda_F = 20.0$, red dots, respectively. The gate energy we used is $E/E_F = 1.0$.

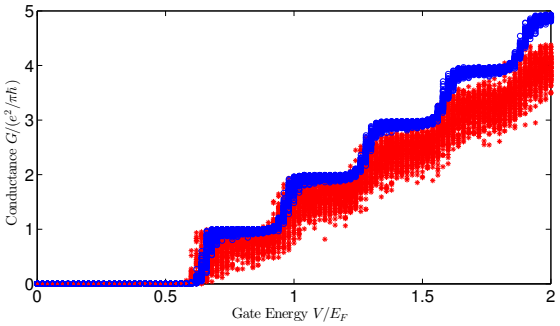

Fig. 7. Examples of the conductances through a quantum point contact as a function of the gate energy under the effect of short-range disorders characterized by the mean free path Λ. Here we show 100 realizations of the random disorders with $\Lambda/\lambda_F = 200.0$, blue dots, and $\Lambda/\lambda_F = 20.0$, red dots, respectively. The bottom energy we used is $V/E_F = 0.5$.

IV. Conclusion

We study the transport properties of a quantum point contact under a confinement. We calculate the conductance of the device with the change of the bottom energy and gate energy. We see that the quantum conductance are quantized for a relative long device. However, the quantization becomes unclear as we decrease the length of the device. We also study the partial transport of each channel in the device. The results show that each channel can contribute one unity of conductance at best. The higher the gate voltage is, the more the transport channels are. At last, we study the effects of short-range disorders on the transport behavior. As expected, the disorder makes an overall decrease of the conductance and makes the quantization less obvious.

Acknowledgment

G.-L. Wang would like to thank Prof. Richard Akis for helpful discussion. And thank Prof. Dragica Vasileska for her wonderful lectures in ASU EEE532, Spring 2015.

References

[1] T. Ando, "Quantum point contacts in magnetic fields," *Phys. Rev. B*, vol. 44, pp. 8017–8027, Oct 1991. [Online]. Available: http://link.aps.org/doi/10.1103/PhysRevB.44.8017

[2] P. A. Khomyakov, G. Brocks, V. Karpan, M. Zwierzycki, and P. J. Kelly, "Conductance calculations for quantum wires and interfaces: Mode matching and green's functions," *Phys. Rev. B*, vol. 72, p. 035450, Jul 2005. [Online]. Available: http://link.aps.org/doi/10.1103/PhysRevB.72.035450

[3] H. U. Baranger and A. D. Stone, "Electrical linear-response theory in an arbitrary magnetic field: A new fermi-surface formation," *Phys. Rev. B*, vol. 40, pp. 8169–8193, Oct 1989. [Online]. Available: http://link.aps.org/doi/10.1103/PhysRevB.40.8169

[4] K.-F. Berggren and Z.-l. Ji, "Resonant tunneling via quantum bound states in a classically unbound system of crossed, narrow channels," *Phys. Rev. B*, vol. 43, pp. 4760–4764, Feb 1991. [Online]. Available: http://link.aps.org/doi/10.1103/PhysRevB.43.4760

[5] T. Ando, "Edge states in quantum wires in high magnetic fields," *Phys. Rev. B*, vol. 42, pp. 5626–5634, Sep 1990. [Online]. Available: http://link.aps.org/doi/10.1103/PhysRevB.42.5626